

Geometries and Energies of Nitrobenzene Studied by CAS-SCF Calculations

M. Takezaki, N. Hirota, M. Terazima,* H. Sato,† T. Nakajima,‡ and S. Kato

Department of Chemistry, Graduate School of Science, Kyoto University, Kyoto 606, Japan

Received: March 13, 1997; In Final Form: May 14, 1997[⊗]

Optimized geometries and energies in the ground (S_0) and excited states of nitrobenzene were calculated using the CAS-SCF method. The optimized geometries in the S_1 , S_2 , T_1 , T_2 , and T_3 states are very different from that in the S_0 state. Most significantly, the nitro group is largely bent out of the phenyl plane in the excited states. The potential curves along the nitro rotation coordinate around the C–N bond and the out-of-plane bending mode of the nitro group in the S_0 , S_1 , T_1 , and T_2 states were calculated in relation to the excited states dynamics. It is found that the potential curves along the bending mode in the excited states are very flat compared with that in the S_0 state. The mechanisms for the fast relaxation from the S_1 and T_1 states are discussed based on the ab initio results.

1. Introduction

Nitrobenzene (NB) is a prototype of aromatic nitro compounds, and the electronic properties including the nature of excited states and dynamics have attracted much interest. The characters of the excited states have been investigated mostly from the absorption spectra in various solvents. For example, the character,^{1,2} and dipole moments^{3–8} of the excited singlet states were estimated from the peak shifts of absorption spectra in several solvents. The lowest excited triplet (T_1) state was assigned to be of $n\pi^*$ character from the reactivity,⁹ and the energy of the T_1 state was estimated to be greater than $20.6 \times 10^3 \text{ cm}^{-1}$ using the energy transfer from NB to piperylene.¹⁰ A very weak transient absorption signal of NB was detected. The signal rises within 5 ps and decays with a lifetime of 770 ps in THF, and it was assigned to the T_1-T_n absorption.¹⁰ However, since the absorption spectrum of NB is generally very broad and structureless in any solvent and even in the gas phase, not many details of the excited states have been elucidated. Furthermore, any authentic fluorescence and phosphorescence have not been detected so far. These spectroscopic properties, lack of fluorescence and phosphorescence, weak transient absorption signal, and broad absorption spectra, prevent a comprehensive understanding of NB.

Recently, we have conducted photochemical studies on the dynamics of the excited states of NB in several solvents.^{11,12} We have found that the lifetimes of the excited states are surprisingly short (the lifetime of the lowest excited singlet (S_1) state is <10 ps and that of the T_1 state is 400–900 ps in ethanol, water, benzene, and alkanes) and that the quantum yield of the triplet formation is very high (≥ 0.80).^{11,12} Almost all energies of the excited states are released by the nonradiative transitions. Although the dynamics of the photoexcited states became clear from these experiments, the mechanism of the fast nonradiative transitions and the geometries in the excited states are still open to question. In this paper, we report a theoretical study on the geometries and the potential curves of the excited singlet and triplet states to understand the unique relaxation processes of NB.

Previously, several theoretical studies were performed on the ground (S_0) state using ab initio methods.^{13–19} All results show that the optimized structure in the S_0 state is planar with C_{2v}

symmetry, and it is consistent with the structure determined by the X-ray diffractions^{14,20–22} and microwave spectroscopy.²³ Compared with rather extensive studies on the S_0 state, theoretical calculations on the excited states are relatively limited at a crude level. Although the energies calculated by some semiempirical molecular orbital (MO) methods^{1,24–28} are consistent with that estimated from the absorption spectrum of NB, some of them are very different.^{29–31} Even for the S_0 state, one of the semiempirical calculations predicted a heavily deformed structure,³¹ which is now known to be incorrect.^{13–23} More refined calculation is needed to elucidate the excited state dynamics. From the absorption spectrum, it was suggested that the intramolecular charge transfer (CT) character contributes to the excited states of NB.^{1,8} If this is the case, CT configurations should be taken into account in the calculation, and excited states should not be described by a single configuration. The multiconfiguration (MC) SCF method will be required. Hence, we calculated the excited states of NB by using complete active space (CAS)-SCF, and the mechanisms of the fast nonradiative relaxation processes from the excited states are discussed based on the results.

2. Methods

All ab initio calculations of NB were performed using the HONDO program³² with two basis sets. One is the Dunning's (9s, 5p)/[3s, 2p] basis set with a d-polarization function on the nitrogen atom (dzv N* basis set). The other is the Dunning's (9s, 5p)/[3s, 2p] basis set with the d-polarization function on all atoms except hydrogen atoms (dzp basis set). The S_0 and excited states were calculated by the CAS-SCF method. In the CAS-SCF wave function, we chose 11 active orbitals (three π and three π^* orbitals of the phenyl part, and two n, two π , and π^* orbitals of the nitro group) and distributed 12 electrons in these active orbitals. The total number of the configuration state functions (CSF's) are 32 670 on the singlet state and 50 820 on the triplet state with C_1 symmetry. The structures and energies were optimized under a restriction of the C_{2v} , C_s , or C_1 symmetries.

3. Results and Discussion

3.1. Ground State. The energy-optimized geometry in the S_0 state obtained by using the dzv N* basis set is shown in Figure 1a. The ground state is mainly described by the $\dots(1b_1)^2(2b_1)^2(16a_1)^2(11b_2)^2(1a_2)^2(3b_1)^2(2a_2)^2$ electronic configuration. The MOs in the CAS-SCF wave functions are

* Present address: Institute for Molecular Science, Okazaki 444, Japan.

† Present address: Department of Applied Chemistry, Graduate School of Engineering, The University of Tokyo, Tokyo 113, Japan.

⊗ Abstract published in *Advance ACS Abstracts*, June 15, 1997.

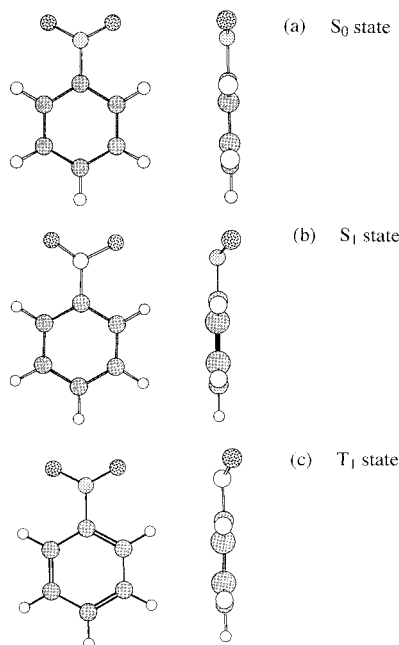


Figure 1. Energy-optimized structures (a) in the S_0 state, (b) in the S_1 state, and (c) in the T_1 state.

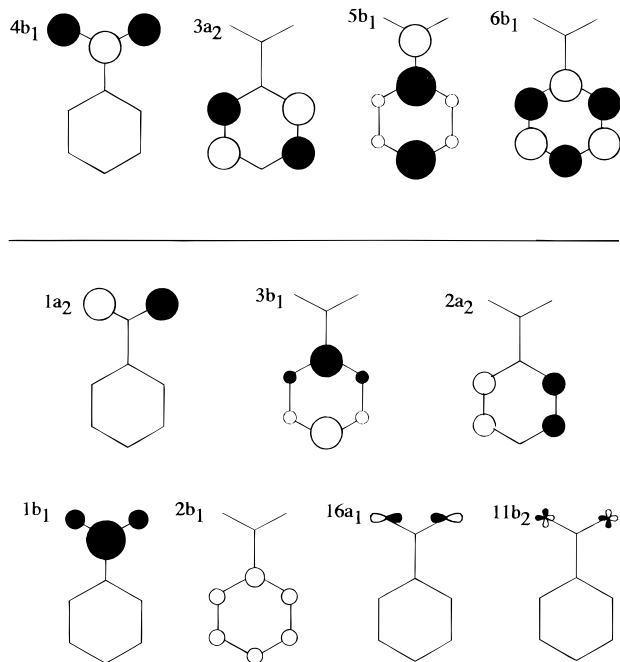


Figure 2. Schematic illustration of MOs of the S_0 state in the CAS-SCF wave functions: (lower) occupied orbitals; (upper) unoccupied orbitals.

schematically illustrated in Figure 2. A planar geometry with the C_{2v} symmetry is predicted using the $dzv N^*$ as well as dzp basis sets, and this geometry is consistent with what was observed experimentally.^{14,20–23} Calculated bond lengths from these basis sets are compared with experimental data^{14,20,21} in Table 1. All bond lengths of both $dzv N^*$ and dzp calculations generally show good agreement with the experimental bond lengths. The dzp calculated dipole moment is 4.275 D, which is in good agreement with the experimental value (4.0,^{3,4} 4.2³ D). Although the $dzv N^*$ calculated dipole moment (4.536 D) is slightly larger than the experimental value, the discrepancy is not so large. From these results, we may conclude that the dzp calculation, as well as the $dzv N^*$ calculation, has sufficient accuracy. In this paper, we mostly use the $dzv N^*$ basis for

TABLE 1: Bond Lengths (Å) of NB in the S_0 State

	dzp	$dzv N^*$	exptl ^a	<i>b</i>	<i>c</i>
C–C ^d	1.398	1.404	1.399	1.387	1.385
C–H ^d	1.074	1.070	1.093	0.9648	
C–N	1.465	1.465	1.486	1.467	1.486
N–O ^d	1.209	1.219	1.223	1.227	1.363

^a In the gaseous phase by the electron diffraction (ref 14). ^b In crystal by X-ray diffraction (ref 20). ^c In crystal by X-ray diffraction (ref 21). ^d Average of bond lengths.

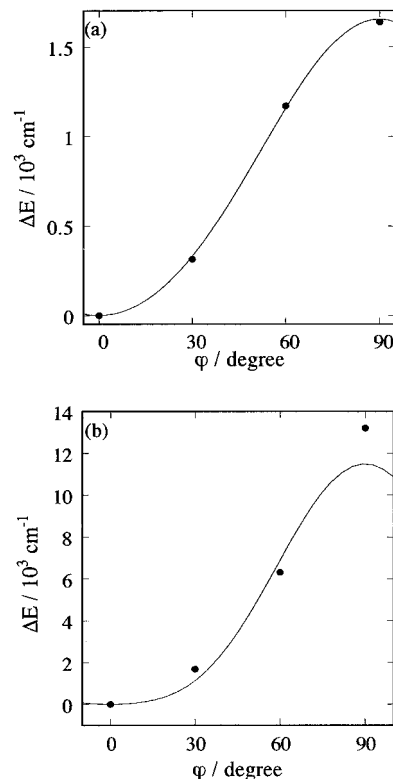


Figure 3. Internal rotational potential curves of the nitro group (a) in the S_0 state and (b) in the T_1 state.

the geometrical optimizations and the energy calculations. Use of the $dzv N^*$ basis reduces the computing time considerably compared with the dzp basis. For the S_1 , T_1 , and T_2 states, which are important for discussing the relaxation processes, the energy calculation with the dzp basis was also performed at the optimized geometries of the $dzv N^*$ calculations.

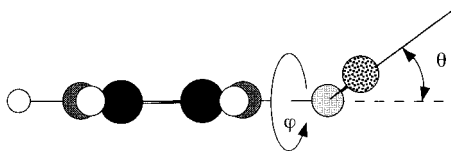
The energies at several rotational angles of the nitro group around the C–N bond with the fixed geometry for the phenyl and nitro parts in the S_0 state are calculated. This potential curve is interesting because of three reasons. First, the geometry and potential curve along vibrational coordinates provide essential information for discussing the dynamics in the excited states. The potential curve along the rotation of the nitro group around the C–N bond might be important for determining the short lifetimes of the excited states. Second, many studies on the intramolecular CT character are concerned with the structure along this coordinate,^{1,31} and the potential curve is a piece of important information. Third, this internal rotational mode have interested researchers experimentally and theoretically in relation to the bond character of C–NO₂.^{8,13,15,23,31,33} The energies calculated at four different rotational angles of φ are shown in Figure 3. The rotational potential curve with a two-site rotor can be conveniently expressed in terms of a Fourier series by¹³

$$V = \sum_n \frac{1}{2} V_{2n} [1 - \cos(2n\varphi)] \quad (1)$$

TABLE 2: Bond Lengths (Å) of NB in Electronically Excited States^a

	S ₁	S ₂	S ₃	T ₁	T ₂	T ₃
C–C	1.404	1.405	1.441	1.404	1.405	1.404
C–H	1.071	1.070	1.069	1.070	1.070	1.071
C–N	1.433	1.450	1.441	1.445	1.427	1.453
N–O	1.381 1.252	1.374	1.223	1.318	1.313	1.371

^a The bond lengths except N–O in the S₁ state are averaged lengths for all corresponding bonds.

**Figure 4.** Labeling of the bending and rotational angles.

where n is an integer and V_{2n} is the $(2n)$ th Fourier coefficient. In many cases, only V_2 and V_4 are sufficient to express the rotational potential curve. V_2 represents the barrier height of the rotational potential and V_4 the shape of the potential curve.¹³ V_2 and V_4 determined by the fitting of our calculated energies (Figure 3) are 1651.7 and -112.3 cm^{-1} , respectively. (The energy difference between the planar and orthogonal structures along the nitro rotation is 1636 cm^{-1} .) This barrier height is reasonably close to the measurement from the microwave spectroscopy, 1000 ± 500 cm^{-1} .²³

3.2. Excited Singlet States. Figure 1b shows the energy-optimized geometry in the S₁ state. The optimized geometry of the S₁ state is strongly distorted from the planar C_{2v} symmetrical form. The most striking feature is the large bending of the nitro group from the phenyl plane (about 33°). Another significant change from that of the S₀ state is a relatively large difference in the two N–O bond lengths. One N–O bond is 0.013 nm longer than the other bond. The nitro group does not rotate along the C–N bond in this optimized structure. Although the phenyl ring is not planar any more, the deviation from the planar form is very small. In Table 2, the bond lengths in the S₁ and other excited states are listed. The bending angles of the nitro group θ (Figure 4), the calculated energies, and the dipole moments of the energy-optimized S₀ and excited states are summarized in Table 3.

The S₁ state calculated with an assumption of the planar C_{2v} symmetrical form is of pure $n\pi^*$ character. The 1^1A_2 state is mainly described by the singly excited configuration from $11b_2$ to $4b_1$ orbitals and is localized mainly at the nitro group. This character is consistent with the previous assignment from the very small absorption coefficient ($\epsilon \approx 130$ $\text{cm}^{-1} \text{M}^{-1}$ in hexane at 330 nm).^{1,2} However, since the nitro group deviates from the phenyl plane, $\pi\pi^*$ character, coming from the $(1a_2)^1(4b_1)^1$ excited configuration with C_{2v} symmetry, is mixed into the S₁ state and this excitation is mainly localized at the nitro group. Figure 5 shows the main contribution of the excitation in the optimized S₁ state. In the optimized S₁ state (C_1 symmetry), $n\pi^*$ and $\pi\pi^*$ states are completely mixed.

Evidently, from Figure 5a, the excitation is heavily localized on the nitro group. The contribution of the charge separation between the nitro and phenyl parts is very small in the optimized S₁ state. The bond lengths of C–C, C–H, and N–C do not change compared with those in the S₀ state. However, the N–O bond lengths become longer with the excitation. These longer N–O bonds are due to the antibonding character of the π^* MO.

The energy difference between the S₀ and S₁ states at the optimized geometries is calculated to be $23\,122$ cm^{-1} by the dzv N* calculation and $24\,593$ cm^{-1} by the dzp calculation.

The energy is about 4000 – 2000 cm^{-1} lower than the experimentally estimated value from the absorption spectrum ($(26$ – $27) \times 10^3$ cm^{-1}).^{1,2} A part of this discrepancy may come from the experimental uncertainty, which is due to the broad feature of the absorption spectrum. The other reason for the discrepancy may be due to the insufficient treatment of the dynamic electron correlation effect in our calculations. The dipole moment of the energy-optimized S₁ state is 3.704 D, which is about 0.3 D lower than the experimental value (4.0 D).³

The character of the S₁ state has been a long-standing question experimentally^{1–3} and theoretically.^{1,2,24,25} The absorption spectrum of this state is usually very broad and structureless even in the gas phase.^{1,2} The solvent shift of the absorption band is opposite that expected for an ordinary $1n\pi^*$ state.³⁴ These peculiar features might be explained by the heavily deformed structure in the S₁ state and the mixed $n\pi^*$ and $\pi\pi^*$ character. For example, the very different structures between the S₀ and S₁ states should be the cause of the broad absorption spectrum.

The calculation with a restriction of the planar geometry (C_{2v} in Table 3) shows that the energy difference between the $-\text{NO}_2$ bent structure and the $-\text{NO}_2$ planar structure is not large (only ~ 1000 cm^{-1}); that is, the potential along the distortion of the nitro group out of the phenyl plane is relatively flat. Compared with this relatively flat potential curve along the bending coordinate, the energy of the perpendicular configuration of the nitro group along the rotation around C–N ($\varphi = 90^\circ$) is about $15\,000$ cm^{-1} higher than that of the planar C_{2v} symmetrical form. This large barrier height in the S₁ state may reflect the partial double bond character of the C–N bond.

The energy optimization of the geometry in the S₂ state was performed with a restriction of the C_s symmetry. The phenyl ring is not planar, but the deviation from the plane is very small. In the optimized S₂ state, $n\pi^*$ and $\pi\pi^*$ states are also completely mixed and are mainly described by the combination of the doubly excited configurations that correspond to the excitations from the $1b_1$ and $16a_1$ to $4b_1$ and from $1a_2$ and $11b_2$ to $4b_1$ orbitals with C_{2v} symmetry. The excitation is also localized mainly at the nitro group (Figure 5b) and makes the N–O bonds longer than those in the S₀ state. The C–C bonds lengths are very similar to those in the S₀ state. In the optimized S₂ state, contribution of the CT configurations is negligibly small, and the weight of CT configuration is less than 0.01 in the wave function.

The optimized geometry of the S₃ state is planar and holds the C_{2v} symmetry even by a calculation under a restriction of the C_s symmetry. The energy-optimized S₃ state from our calculation is a $\pi\pi^*$ state and is mainly described by the singly excited configurations, the $(2a_2)^1(5b_1)^1$ and $(2a_2)^1(4b_1)^1$, which are similar to the first excited state of benzene. The excitation occurs mainly at the phenyl ring and is almost delocalized over the NB molecule (Figure 5c). The C–C bond lengths become longer than those in the S₀ state. On the other hand, the N–O bonds lengths are similar to those in the S₀ state. This state could be the experimentally observed $1^1\pi\pi^*$ state. However, from the solvent effect on the absorption spectra, a large contribution (about 50%) of the CT character has been suggested for this state.¹ On the other hand, from our calculated MO, the contribution of the CT configuration in this state is found to be very small, and the weight of CT configurations is less than 0.05 in the wave function. The experimentally observed CT state having a large dipole moment could be located near but higher than the S₃ state ($\sim 37\,000$ cm^{-1}). Within our calculated energy range, we could not find any CT state.

3.3. Excited Triplet States. Figure 1c shows the energy-optimized geometry of the T₁ state without any symmetrical

TABLE 3: Properties of NB Calculated with dzv N* Basis^g

state	symmetry/geometrical restriction	character	θ/deg	$E_{\text{cal}}^a/\text{cm}^{-1}$	$E_{\text{exp}}/\text{cm}^{-1}$	$\mu_{\text{cal}}/\text{D}$	$\mu_{\text{exp}}/\text{D}$
S ₀	C_{2v} , $1^1A_1/C_s$		0.0	0 (0)		4.536	4.0, ^e 4.2 ^f
S ₁	C_1/C_1	$(n, \pi) \rightarrow \pi^*$	32.8	23 122 (24 593)	~27000 ^b	3.704	4.0 ^f
	C_s , $1^1A''/C_s$	$(n, \pi) \rightarrow \pi^*$	39.6	23 764		3.449	
	C_{2v} , $1^1A_2/C_{2v}$	$n \rightarrow \pi^*$	0.0	24 175		3.605	
	C_s , $1^1A'/C_s$	$(n, \pi) \rightarrow \pi^*$	62.8	27 861		2.675	
S ₂	C_{2v} , $2^1A_2/C_s$	$\pi \rightarrow \pi^*$	0.0	37 160	~35000 ^c	4.700	9.0 ^f
T ₁	C_s , $1^3A''/C_s$	$(n, \pi) \rightarrow \pi^*$	38.8	18 360 (20 290)	$(22-27) \times 10^3$ ^d	2.798	
	C_{2v} , $1^3B_2/C_{2v}$	$\pi \rightarrow \pi^*$	0.0	19 030		2.601	
T ₂	C_s , $2^3A''/C_s$	$(n, \pi) \rightarrow \pi^*$	33.4	22 905 (24 508)		3.508	
	C_{2v} , $1^3A_2/C_{2v}$	$n \rightarrow \pi^*$	0.0	23 009		3.646	
T ₃	C_s , $1^3A'/C_s$	$(n, \pi) \rightarrow \pi^*$	54.2	27 142		2.761	

^a Energy differences between the S₀ and excited states at the optimized geometries. ^b Estimated from the steady state absorption spectrum (refs 1 and 2). ^c Estimated from the steady state absorption spectrum (ref 1). ^d References 11 and 12. ^e References 3 and 4. ^f Reference 3. ^g The energies calculated with the dzp basis are shown in the parentheses for E_{cal} .

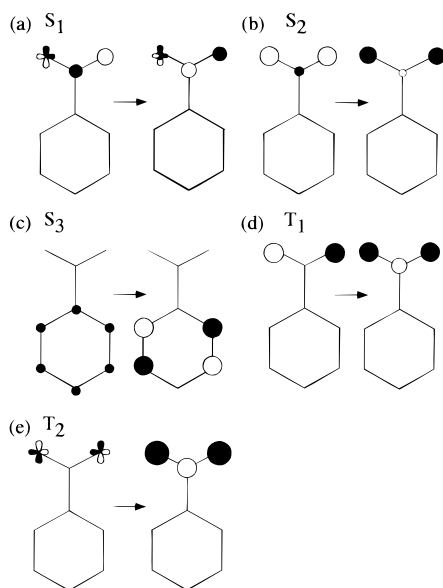


Figure 5. Schematic representations of the main contributions of the excitations in the (a) S₁, (b) S₂, (c) S₃, (d) T₁, and (e) T₂ states.

restriction. The two N–O distances are the same at the optimized structure of the T₁ state, in contrast to those in the S₁ state. Thus, the T₁ state is of C_s symmetry. The phenyl ring is almost planar. The nitro group is largely bent from the phenyl plane (about 39°). The calculation using a C_{2v} symmetrical restriction (C_{2v} in Table 3) shows that the energy difference between the restricted (planar C_{2v} symmetry) and unrestricted (the nitro group bent) geometries is very small (only 670 cm⁻¹). The calculated energy difference between the S₀ and T₁ states is 18 360 cm⁻¹ with the dzv N* basis and 20 290 cm⁻¹ with the dzp basis, the energy by the dzp calculation being closer to the experimentally measured energy.^{11,12}

The T₁ state was assigned to be of ${}^3n\pi^*$ character from a photochemical study,⁹ but owing to the largely bent structure of the nitro group, the calculated T₁ state is of $n\pi^*$ and $\pi\pi^*$ mixed character (Figure 5d). The excitation is mainly localized at the nitro group. It is interesting to note that the T₁ state calculated with a restriction of the C_{2v} symmetry (planar form) is a pure ${}^3\pi\pi^*$ state, 1^3B_2 , which is described by the singly excited configuration from the $1a_2$ to $4b_1$ orbitals localized mainly on the nitro group. A pure ${}^3n\pi^*$ state, localized mainly at the nitro group, coming from the $(11b_2)^1(4b_1)^1$ excited configuration with C_{2v} symmetry, 1^3A_2 , is located about 4500 cm⁻¹ higher than the optimized T₁ state. To examine the correlation between the pure (${}^3\pi\pi^*$ and ${}^3n\pi^*$) states and the geometry-optimized (T₁ and T₂) states, the energies at several

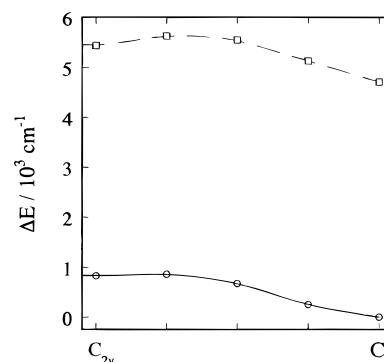


Figure 6. Potential curves of the T₁ (○) and T₂ (□) structures from C_{2v} to C_s forms. The broken and solid lines are only a guide for the eyes.

intermediate geometries between the optimized C_{2v} and C_s geometries are calculated (Figure 6). Both curves do not show a distinct avoided crossing and lead to the T₁ and T₂ states of the bent structure. Therefore, we conclude that the optimized T₁ state is correlated with the ${}^3\pi\pi^*$ state of the planar structure. The ${}^3n\pi^*$ character is mixed in the T₁ state by the large bending from the planar structure. In the T₁ state (Figure 5d), the ${}^3\pi\pi^*$ character seems to be larger than the ${}^3n\pi^*$ character.

The excitation is mainly localized at the nitro group (Figure 5d) in the T₁ state. Owing to the localized excitation, the N–O bonds become longer than those in the S₀ state, but the C–C bond lengths are similar to those of the S₀ state. Sometimes the excited state character of NB is discussed in relation to the intramolecular CT character. However, the calculated wave function does not show such a CT character in the T₁ state, and the weight of CT configuration is less than 0.01 in the wave function. This lack of CT character is consistent with the previous experimental observation: the triplet lifetime does not depend much on the polarity of the solvent.¹¹

The energies at several rotational angles with a fixed geometry for the phenyl ring and a nitro group in the T₁ state are calculated and are shown in Figure 3b. The Fourier coefficients of the internal rotational potential curve of the nitro group in the T₁ state are obtained as $V_2 = 12 294$ and $V_4 = -2661$ cm⁻¹, although the fitting by eq 1 is rather poor (Figure 3b). Equation 1 holds well for a simple two-site rotor where the rotational axis is the same as the C₂ axis. In this NB case, since the T₁ state has no symmetrical axis, eq 1 could not be applicable. However, the energy difference between the optimized and orthogonal structures is 13 202 cm⁻¹ and not much different from V_2 . This barrier height along the rotation of the nitro group in the T₁ state is about 8–9 times higher than that in the S₀ state.

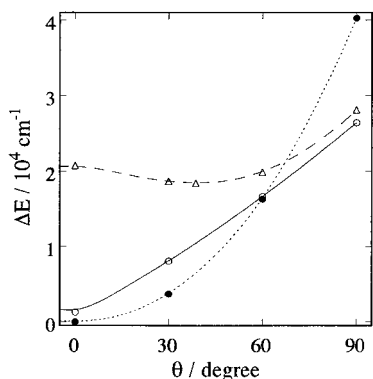


Figure 7. Calculated energies at various bending angles (θ). Open and closed circles represent the energies in the S_0 state. The structural parameter except θ is fixed to the optimized structure in the T_1 (\circ) and the S_0 (\bullet) states. Triangles represent the energy in the T_1 state. The structural parameter except θ is fixed to the optimized structure in the T_1 state. The lines are only a guide for the eyes.

The optimized geometry of the T_2 state is calculated with the geometrical restriction of the C_s symmetry. The optimized T_2 state is about 4500 and 4000 cm^{-1} higher than the T_1 state by the dzv N* and dzp calculations, respectively. The phenyl ring is again almost planar. The nitro group is bent (33.4°) from the phenyl ring. The excitation is also localized mainly at the nitro group (Figure 5e). As mentioned above, this T_2 state is correlated with the ${}^3\pi\pi^*$ state in the planar form.

The T_3 state is optimized with a geometrical restriction of the C_s symmetry. The nitro group is much largely bent from the phenyl plane (54.2°). The excitation is mainly described by the $(16a_1)^1(4b_1)^1$ singly excited configuration mixed with the $(1b_1)^1(4b_1)^1$ configuration at the C_{2v} symmetry and is mainly localized at the nitro group. The N–O bonds are longer than those in the S_0 state. Within our calculated energy range, we could not find any ${}^3\pi\pi^*$ state localized on the phenyl moiety. Such a ${}^3\pi\pi^*$ state may be located at an energy higher than 27 000 cm^{-1} , and this seems to be reasonable when we consider that the energy of the T_1 state of benzene is 31 456 cm^{-1} .³⁵

3.4. Photophysical Processes in the Excited States. Any fluorescence from NB has not been reported so far. From the transient absorption and the transient grating studies, the lifetime of the S_1 state is determined to be less than 5 ps (or 10 ps) in THF and water.^{10,11} Considering the very efficient $S_1 \rightarrow T_1$ intersystem crossing (isc) ($\Phi_{\text{isc}} \geq 0.8$),^{11,12} the short lifetime of the S_1 state should be attributed to the very fast $S_1 \rightarrow T_1$ isc. Previously, the S_1 and T_1 states were considered as pure $n\pi^*$ states. Hence, it was predicted that the $T_2({}^3\pi\pi^*)$ state should be located between the S_1 and T_1 states^{25,26} and the direct spin–orbit coupling between the S_1 and T_2 states could be responsible for the fast isc. However, in this study, we found that all of the S_1 , T_1 , and T_2 states are heavily mixed with $n\pi^*$ and $\pi\pi^*$ character. Moreover, the T_2 state is found to be very close to the S_1 state (90–200 cm^{-1}). Indeed, if we calculate the energy of the T_2 state with the optimized geometry of the S_1 state, the energy is slightly higher ($\sim 200 \text{ cm}^{-1}$) than that of the S_1 state. It suggests that the potential curve of the T_2 state along the nitro bending mode crosses that of the S_1 state near the bottom of the curve. This potential crossing should enhance the coupling between the S_1 and T_2 states dramatically and increase the $S_1 \rightarrow T_2$ isc rate. The population in the T_2 state should relax to the T_1 state quickly by vibrational relaxation and internal conversion (ic) process.

The other interesting feature in the photophysics of NB is the very short lifetime of the T_1 state (e.g., 480 ps in ethanol at room temperature).¹¹ Compared with the microsecond to

millisecond lifetimes of the T_1 states for many organic molecules, the $T_1 \rightarrow S_0$ isc is 10^3 – 10^6 times more efficient. This efficient $T_1 \rightarrow S_0$ isc should be related to the geometry and the potential curve of the T_1 state.

The energies of the S_0 and T_1 states at various bending angles of the nitro group were calculated and are shown in Figure 7. For simplicity, the geometry of the phenyl ring was fixed to the optimized geometry in the T_1 state. Since the energy difference between $\theta = 0^\circ$ (planar structure) and $\theta = 39^\circ$ (optimized structure) and that between $\theta = 60^\circ$ and $\theta = 39^\circ$ in the T_1 state are not large (1590 and 2320 cm^{-1}), the nitro group can easily fluctuate along the bending mode. On the other hand, the energy along the bending mode in the S_0 state increases sharply with an increase in the bending angle from $\theta = 0^\circ$. At $\theta = 60^\circ$ the energetic difference between the S_0 and T_1 state is only 3000 cm^{-1} . (If we calculate the potential curve of the S_0 state with the optimized phenyl geometry in the S_0 state, both potential curves cross at $\theta = 70^\circ$ (Figure 7).)

The dramatic difference in the curvature of the potential curve between the T_1 and S_0 states makes the Franck–Condon (FC) factor large for the $T_1 \rightarrow S_0$ isc. A similar mechanism for the fast radiationless transition was proposed for the $T_1 \rightarrow S_0$ isc of pyridazine (1,2-diazabenzene).³⁶ In the pyridazine case, a theoretical calculation predicted that the curvature for the potential curve along the twisting mode of the N=N bond in the T_1 state is much smaller than that in the S_0 state even though the most stable geometries in the T_1 and S_0 states are very similar. The very different curvature makes the triplet lifetime very short (~ 100 ns at room temperature)³⁷ compared with those of the other azaaromatics. In the NB case, the bent structure of the nitro group is actually the most stable one. The heavily deformed structure, very close potential curves between the S_0 and T_1 states at $\theta > 40^\circ$, and the rather flat potential surface may be the cause of the further short triplet lifetime (~ 480 ps).

The calculated, rather flat potential curve along the bending mode in the T_1 state suggests that the distortion along this coordinate is easily thermally activated. From the higher vibrational level, the FC factor becomes larger and also the energy gap between the T_1 and S_0 states becomes smaller. Considering these two factors, the lifetime of the T_1 state may be temperature dependent if this mechanism of the nonradiative transition is correct. In our previous paper, we reported that the triplet lifetime becomes longer from 480 to 800 ps with decreasing temperature from 298 to 253 K.¹¹ This observation is consistent with the above prediction from the present theoretical calculations.

4. Conclusion

The optimized structures, energies, and dipole moments of the S_0 and excited states of NB were calculated by the CAS-SCF method. Although the structure in the S_0 state is planar with C_{2v} symmetry, the nitro group is largely bent from the phenyl plane in the S_1 , S_2 , T_1 , T_2 , and T_3 states. The S_1 , S_2 , T_1 , T_2 , and T_3 states are of heavily mixed $\pi\pi^*$ and $n\pi^*$ character mainly localized at the nitro group. Interestingly, the T_1 state is correlated with the ${}^3\pi\pi^*$ state localized at the nitro group in the planar structure. Potential curves along the $-\text{NO}_2$ rotation around the C–N bond and along the bending mode to the out-of-plane are calculated for the S_0 , S_1 , T_1 , and T_2 states. The curvature of the potential curve along the bending coordinate is dramatically reduced on going from the S_0 state to the excited states, while the potential curve along the rotational coordinate becomes very steep in the excited states. Both potential curves of the S_1 and T_2 states should cross near the bottom of the potential curve of the S_1 state. This crossing should cause a

very fast decay of the S_1 state. The very different geometries and the different curvatures between the S_0 state and the excited states can be the cause of the very efficient $T_1 \rightarrow S_0$ isc processes. The thermally activated out-of-plane bending motion of the nitro group could control the $T_1 \rightarrow S_0$ isc process, and that is consistent with the experimentally observed temperature dependence of the T_1 lifetime.

Acknowledgment. Some of the present calculations were carried out at the Data Processing Center, Kyoto University. This work was supported by the Grants in Aid from the Ministry of Education, Science, and Culture in Japan.

References and Notes

- (1) Nagakura, S.; Kojima, M.; Maruyama, Y. *J. Mol. Spectrosc.* **1964**, *13*, 174.
- (2) Vidal, B.; Murrell, J. N. *Chem. Phys. Lett.* **1975**, *31*, 46.
- (3) Seliskar, C. J.; Khalil, O. S.; McGlynn, S. P. In *Excited States*; Lim, E. C., Ed.; Academic Press: New York, 1974; Vol. 1.
- (4) Prabhumirashi, L. S.; Kunte, S. S. *Spectrochim. Acta* **1986**, *42A*, 435.
- (5) Prabhumirashi, L. S.; Kunte, S. S. *Spectrochim. Acta* **1988**, *44A*, 213.
- (6) Prabhumirashi, L. S. *Spectrochim. Acta* **1983**, *39A*, 91.
- (7) Prabhumirashi, L. S.; Kutty, D. K. N.; Bhide, A. S. *Spectrochim. Acta* **1983**, *39A*, 663.
- (8) Sinha, H. K.; Yates, K. *J. Chem. Phys.* **1990**, *93*, 7085.
- (9) Hurley, R.; Testa, A. C. *J. Am. Chem. Soc.* **1966**, *88*, 4330.
- (10) Yip, R. W.; Sharma, D. K.; Giasson, R.; Gravel, D. *J. Phys. Chem.* **1984**, *88*, 5770.
- (11) Takezaki, M.; Hirota, N.; Terazima, M. *Phys. Chem.*, in press
- (12) Takezaki, M.; Hirota, N.; Terazima, M. *Prog. Nat. Sci.* **1996**, *6*, S-453.
- (13) Head-Gordon, M.; Pople, J. A. *Chem. Phys. Lett.* **1990**, *173*, 585.
- (14) Domenicano, A.; Schultz, G.; Hargittai, I.; Colapietro, M.; Portalone, G.; George, P.; Bock, C. W. *Struct. Chem.* **1990**, *1*, 107.
- (15) Penner, G. H. *J. Mol. Struct.* **1986**, *137*, 121.
- (16) Shlyapochnikov, V. A.; Khaikin, L. S.; Grikina, O. E.; Bock, C. W.; Vilkov, L. V. *J. Mol. Struct.* **1994**, *326*, 1.
- (17) Bock, C. W.; Trachtman, M.; George, P. *J. Mol. Struct.* **1985**, *122*, 155.
- (18) Politzer, P.; Lane, P.; Jayasuriya, K.; Domelsmith, L. N. *J. Am. Chem. Soc.* **1987**, *109*, 1899.
- (19) Ritchie, J. P. *Tetrahedron* **1988**, *44*, 7645.
- (20) Boese, R.; Bläser, D.; Nussbaumer, M.; Krygowski, T. M. *Struct. Chem.* **1992**, *3*, 363.
- (21) Trotter, J. *Tetrahedron* **1960**, *8*, 13.
- (22) Trotter, J. *Acta Crystallogr.* **1959**, *12*, 884.
- (23) Hog, J. H.; Nygaard, L.; Sørensen, G. O. *J. Mol. Struct.* **1970**, *7*, 111.
- (24) Sieiro, C.; Fernández-Alonso, J. I. *Chem. Phys. Lett.* **1973**, *18*, 557.
- (25) González-Lafont, A.; Lluch, J. M.; Bertrán, J.; Marquet, J. *Spectrochim. Acta* **1988**, *44A*, 1427.
- (26) Kiss, A. I.; Szöke, J. *J. Mol. Struct.* **1973**, *18*, 457.
- (27) Dirk, C. W.; Kuzyk, M. G. *Phys. Rev. A* **1989**, *39*, 1219.
- (28) Cucchiara, G.; Dovesi, R.; Ricca, F.; Cerruti, L. *J. Mol. Struct.* **1978**, *43*, 61.
- (29) Bigelow, R. W.; Freund, H. J.; Dick, B. *Theor. Chem. Acta* **1983**, *63*, 177.
- (30) Cucchiara, G.; Dovesi, R.; Ricca, F.; Cerruti, L. *J. Mol. Struct.* **1978**, *43*, 61.
- (31) Malar, E. J. P.; Jug, K. *J. Phys. Chem.* **1984**, *88*, 3508.
- (32) Dupuis, M.; Watts, J. D.; Villar, H. O.; Hurst, G. J. B. HONDO, Version 7.0. *QCPE* **1987**, 544.
- (33) Ribeaud, M.; Bauder, A.; Günthard, H. H. *Mol. Phys.* **1972**, *23*, 235.
- (34) Balasubramanian, A.; Rao, C. N. R. *Spectrochim. Acta* **1962**, *18*, 1337.
- (35) Ziegler, L. D.; Hudson, B. S. In *Excited States*; Lim, E. C., Ed.; Academic Press: New York, 1982; Vol. 5.
- (36) Terazima, M.; Yamauchi, S.; Hirota, N.; Kitao, O.; Nakatsuji, H. *Chem. Phys.* **1986**, *107*, 81.
- (37) Terazima, M.; Hirota, N. *Chem. Phys. Lett.* **1992**, *189*, 560.